Hindawi Publishing Corporation
Journal of Nanomaterials
Volume 2015, Article ID 530631, 8 pages
http://dx.doi.org/10.1155/2015/530631

Research Article

Sythesis, Modification, and Biosensing Characteristics of Au_2S/AuAgS-Coated Gold Nanorods

Yanting Liu,[1] Yanan Ma,[1] Jun Zhou,[1] Xing Li,[2] Shusen Xie,[3] and Ruiqin Tan[4]

[1]*Institute of Photonics, Faculty of Science, Ningbo University, Ningbo, Zhejiang 315211, China*
[2]*School of Materials Science and Chemical Engineering, Ningbo University, Ningbo, Zhejiang 315211, China*
[3]*Fujian Provincial Key Laboratory for Photonics Technology, Key Laboratory of Optoelectronic Science and Technology for Medicine of Ministry of Education, Fujian Normal University, Fuzhou 350007, China*
[4]*School of Information Science and Engineering, Ningbo University, Ningbo, Zhejiang 315211, China*

Correspondence should be addressed to Jun Zhou; zhoujun@nbu.edu.cn

Received 2 October 2014; Revised 6 January 2015; Accepted 20 January 2015

Academic Editor: Amir Kajbafvala

The Au_2S/AuAgS-coated gold nanorods (Au_2S/AuAgS/GNRs) are prepared by a facile synthesis method and functionally modified for their biosensing application. In the preparation process, the longitudinal plasmon resonance (LPR) bands of Au_2S/AuAgS/GNRs can be changed by controlling the thickness of the chalcogenide layer coated on GNRs. Especially, the LPR band located at 800 nm is obtained for biosensing application in the near-infrared region. Furthermore, mercaptoundecanoic acid (MUA) and poly(styrenesulfonate) (PSS) are, respectively, used to modify Au_2S/AuAgS/GNRs to acquire the functional nanoprobes; that is, MUA-modified and PSS-modified Au_2S/AuAgS/GNRs and their different chemical reaction mechanisms are studied by the absorption spectrum and ξ-potential measurement. Then, the functional nanoprobes are incubated with anti-prostate-specific antigen (PSA) antibody to detect PSA. The experimental results demonstrate that the functional nanoprobes are sensitive to the target binding of PSA. Therefore, Au_2S/AuAgS/GNRs are suitable to form the bioprobes for detection of PSA in early-phase prostate cancer.

1. Introduction

Noble metal nanoparticles (mainly Ag, Au, Pd, and Pt) have attracted more attentions due to their distinct physical and chemical properties, such as the quantum effect, the small size effect, large surface-to-volume ratio, and high surface chemical activity [1, 2]. Among them, gold nanoparticles have been widely used in biological and optical sensing [3], cancer imaging [4], chemical catalysis [5], and message storage [6, 7], which is ascribed to their localized surface plasmon resonance (LSPR) and biocompatibility properties. In particular, over the past decade, many groups have focused their researches on the synthesis mechanism, surface functionality, and relative biological application of gold nanorods (GNRs) [8–11]. It is because the LSPR properties of GNRs are easily tuned by simply changing the aspect ratio of the nanorods besides their high optical absorption cross sections and great molar extinction coefficients in ultraviolet-visible region. Compared with gold nanospheres, GNRs are commonly characterized by two principal plasmon absorption bands, corresponding to the transverse plasmon resonance (TPR) and the longitudinal plasmon resonance (LPR) modes which are from the oscillation of conduction electrons [8, 9]. And the LPR band of GNRs is highly sensitive to the refractive index change of surrounding medium, which has been developed into an effective exploiter of biosensors [12–14].

On the other hand, many methods have been reported for preparing GNRs, for example, lithographic fabrication, template-assessed synthesis, and ultraviolet photochemical reduction of the gold salts [15–17]. In fact, the most usual way to synthesize GNRs is the wet chemical seed-growth method due to its advantages of the facile operation and the mild aqueous reaction conditions [18, 19]. More importantly, by using the seed-mediated approach, the size and morphology of GNRs can be tailored by varying the ratio of seed to metal salt or coating other materials on the surface of

the GNRs [8, 9]. As a result, the LSP band of GNRs can be tuned in a wide wavelength region [20, 21]. As we know, plasmonic sensors based on the LSPR characteristics of GNRs are highly sensitive to the changes of refractive index caused by molecular interactions in the vicinity of the GNRs [22]. As reported [23], the absorption band of the GNRs with high-aspect-ratio is located in the "window of optical transparency," that is, in near-infrared region of 700–900 nm, which can achieve stronger optical absorbance and greater tissue penetration [23, 24]. However, it is cost-consuming and requires the strict synthesis conditions to obtain the GNRs with high-aspect-ratio [25, 26]. Therefore, it is crucial to adjust the surface plasmon resonance band of GNRs to near-infrared region for their promising biological application.

In this paper, we provided a facile way to modulate the localized surface plasmon resonance band of gold nanorods into near-infrared region by coating a chalcogenide layer on the surface of gold nanorods, namely, Au_2S/AuAgS-coated gold nanorods (Au_2S/AuAgS/GNRs). And the synthesis mechanism of the hybrid nanorods was discussed in detail. Then, to the functionalization of Au_2S/AuAgS/GNRs, mercaptoundecanoic acid (MUA) and poly(styrenesulfonate) (PSS) separately modified the surface of CTAB-stabilized GNRs. Finally, the above functionalized Au_2S/AuAgS/GNRs were incubated with anti-prostate-specific antigen (PSA) antibody to form the nanoprobe for detecting PSA in aqueous solution. As a consequence, the functionalized Au_2S/AuAgS/GNRs showed an excellent performance as a label-free nanosensor platform for early-phase diagnosis of disease progression based on LSPR characteristics.

2. Materials and Methods

2.1. Materials. Silver nitrate ($AgNO_3$), sodium borohydride ($NaBH_4$), tetrachloroauric acid ($HAuCl_4 \cdot 3H_2O$), sodium thiosulfate pentahydrate ($Na_2S_2O_3$), N-hydroxysuccinimide (NHS), N-ethyl-N-(dimethylaminopropyl) carbodiimide (EDC), mercaptoundecanoic acid (MUA), and PBS buffer solution were purchased from Sigma Aldrich Reagent Co. Ltd, (St. Louis, USA). Hexadecyltrimethylammonium bromide (CTAB) was obtained from Sinopharm Chemical Reagent Co. (Shanghai, China). Ascorbic acid (AA) was purchased from Bodi Chemical Reagents Co. (Tianjin, China). Poly(styrenesulfonate) ($M_w \approx 14000$) (PSS) was obtained from J&K Chemical. Prostate-specific antigen (PSA) and anti-PSA antibody were obtained from Shanghai Linc-Bio Science Co. Ltd. Bovine serum albumin (BSA) was purchased from Nanjing Sunshine Biotechnology Co. Ltd. Milli-Q water (18 MΩ cm resistivity) was used for all solution preparations. Glasswares were cleaned by aqua regia and rinsed with deionized water prior to the experiment.

2.2. Synthesis of GNRs. The gold NRs were prepared by using a seed-mediated growth method [8, 9] in aqueous solutions. Briefly, the seed solution was generated by adding ice-cold $NaBH_4$ (0.60 mL, 0.01 M) aqueous solution to the mixture solution of $HAuCl_4$ (0.25 mL, 0.01 M) and CTAB (7.5 mL, 0.1 M), followed by rapid inversion mixing for 2 min into a brown yellow solution. The growth solution, containing CTAB (47.5 mL, 0.1 M), $HAuCl_4$ (2 mL, 0.01 M), $AgNO_3$ (0.30 mL, 0.01 M), and AA (0.32 mL, 0.1 M), was prepared and then immediately changed to colorless after the AA was added. Finally, 0.1 mL seed solution was added to the growth solution and the reaction mixture was gently agitated for 20 s and left undisturbed overnight.

2.3. Preparation of Au_2S/AuAgS/GNRs. Based on the research work of Huang et al. presented in [27, 28], a modified strategy is used to coat a chalcogenide layer on the surface of GNRs. The Au_2S/AuAgS/GNRs were prepared by adding $Na_2S_2O_3$ (0.055 mL, 1.0 M) solution into 5 mL of the as-synthesized gold nanorods at room temperature, heated, and kept at 50°C with different reaction time ranging from 20 s to 3 h. Then the mixture of GNRs and $Na_2S_2O_3$ was taken out, cooled to room temperature, followed by centrifugation at 10000 rpm for 20 min, and redispersed in 5 mL water. In our experiments, the as-prepared Au_2S/AuAgS/GNRs were highly dispersed in water without aggregation during several weeks.

2.4. Modification of Au_2S/AuAgS/GNRs. The surface modification of Au_2S/AuAgS/GNRs was carried out with MUA and PSS, respectively. In brief, MUA (0.6 mL, 0.01 M) ethanol solution was added into the 5 mL purified Au_2S/AuAgS/GNRs for reacting for 20 h. Then the modified nanorods were washed by centrifugation and resuspended in 5 mL water. The PSS monolayer was formed on the Au_2S/AuAgS/GNRs by mixing PSS (0.5 mL, 0.01 M) solution with the 5 mL hybrid nanostructures and then rinsed by centrifugation at 10000 rpm for 20 min and resuspended in 5 mL water.

2.5. Immunoassay of PSA. To attach biological molecules on the surface of the modified Au_2S/AuAgS/GNRs, the EDC and NHS solution was firstly added to the modified nanorods and then incubated in an anti-PSA antibody solution (0.02 mg/mL) for 30 min. Then, a blocking solution BSA (0.02 mg/mL) was added to above prepared nanoprobes to shield the bare sites on the surfaces of the modified Au_2S/AuAgS/GNRs, followed by centrifugation at 6000 rpm for 30 min and dispersion in PBS solution. The prepared nanoprobes were further used for detecting PSA.

2.6. Characterization and Measurement. Transmission electron microscope (TEM) images were obtained with the TEM (JEM-2100F, JEOL) operating at an accelerating voltage of 200 kV. And UV-Vis absorption spectra were measured with the spectrometer (TU1901, Pgeneral). ξ-potential measurements were performed with the nanoparticle size analyzer (Zetasizer Nano S90, Malvern). Powder X-ray diffraction (PXRD) data were collected on the Bruker D8 Focus X-ray diffractometer with nickel-filtered Cu Kα1 ($\lambda = 1.54060$ Å) radiation. The calculated PXRD patterns were produced using the SHELXTL-XPOW program. Energy-dispersive X-ray (EDX) spectroscopy was carried out at 5 kV using a SU-70 field-emission scanning electron microscope (SU70, FESEM).

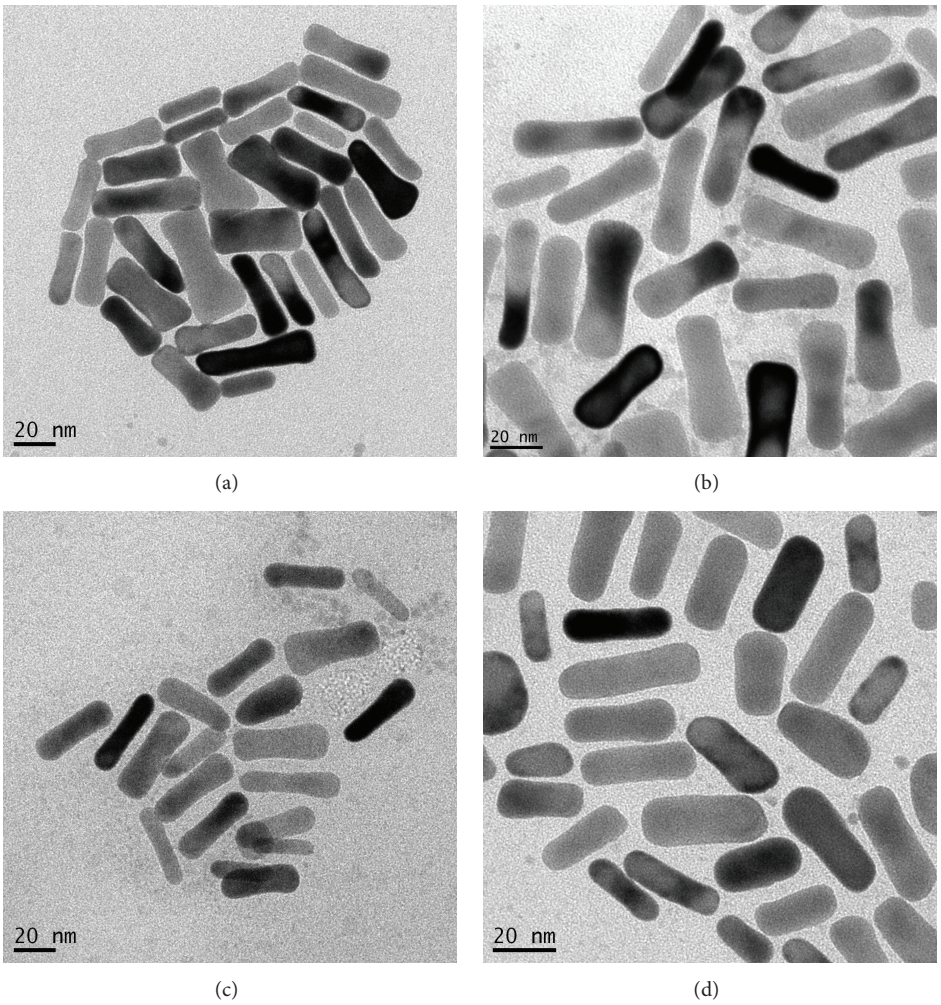

(a) (b) (c) (d)

Figure 1: TEM images of (a) the as-prepared GNRs and ((b)–(d)) as-prepared Au_2S/AuAgS/GNRs under different reaction time (b) 1 min, (c) 15 min, and (d) 30 min.

3. Result and Discussion

3.1. Characterization of GNRs and Au_2S/AuAgS/GNRs. The GNRs were synthesized by the seed-mediated growth method with the help of surfactant-directed shape [8, 9], and their TEM image is shown in Figure 1(a). It is seen that the as-synthesized GNRs have an average aspect ratio of 3.1. The chalcogenide layer is coated on the surface of GNR by mixing an excess of freshly prepared $Na_2S_2O_3$ aqueous solution with the GNRs. Then the gold core-shell nanorods with chalcogenide complexes were obtained and shown in Figures 1(b)–1(d). Comparing their TEM images in Figure 1, it is clear that the average size of the gold nanorods coated with chalcogenide seems to be smaller than that of the original gold nanorods due to the corrosion of gold nanorods. Besides, it is seen from Figures 1(b)–1(d) that the morphologies of the core-shell nanocomposite are fairly uniform in shape and the average aspect ratio of the core-shell nanorods is increased with increasing the reaction times. Thus, it illustrates that the corrosion occurred both at the sides and the ends of gold nanorods and eventually led to the formation of high aspect ratio nanorods, which is different from the conventional formation of core/shell structure by coating the shell on surface of the nanorods.

Moreover, the energy-dispersive X-ray (EDX) spectrum and the powder X-ray diffraction (PXRD) spectrum of the gold nanorods with chalcogenide complexes are shown in Figure 2. As shown in Figure 2(a), it clearly displays that the sample is mainly composed of the elements Au, Ag, and S, and the elements of silicon and bromine are from the silicon substrate and the surfactant CTAB. Meanwhile, the PXRD spectra shown in Figure 2(b) further identify the chalcogenide complexes of Au_2S and AuAgS according to the previous reports [27]. Compared with the PXRD spectrum of GNRs, it is found that the peaks of surfactant CTAB on the surface of GNRs disappeared and a weak peak of the Au_2S/AuAgS complexes arose in the PXRD spectrum of Au_2S/AuAgS/GNRs. Thus, it confirms that the Au_2S/AuAgS/GNRs hybrid nanoparticles are successfully fabricated.

On the other hand, during the preparation process of Au_2S/AuAgS/GNRs, their absorption spectra were recorded

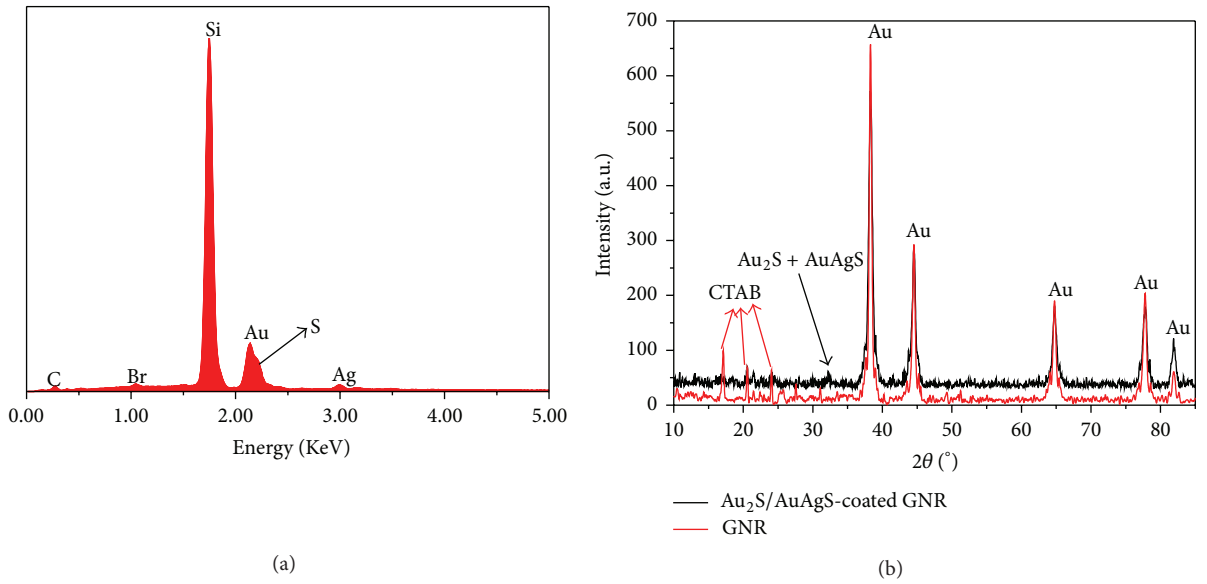

Figure 2: (a) EDX spectrum of Au_2S/AuAgS/GNRs. (b) PXRD spectra of GNRs and Au_2S/AuAgS/GNRs.

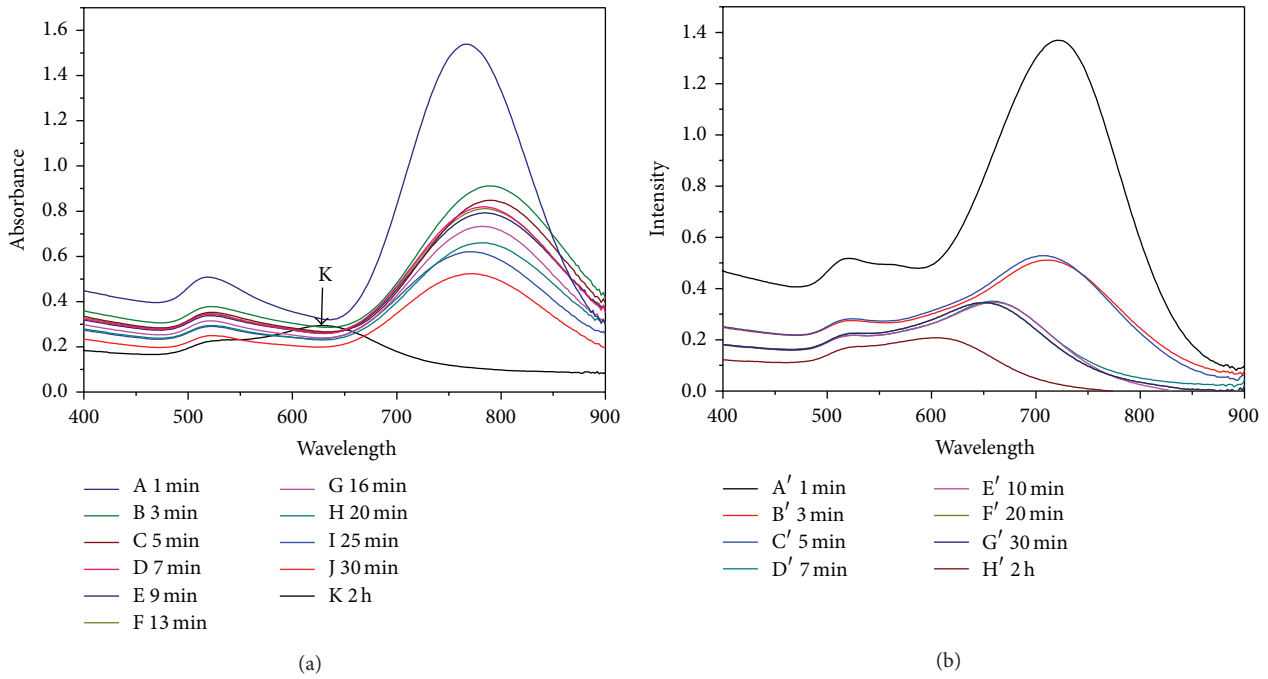

Figure 3: UV-vis-NIR spectra of Au_2S/AuAgS/GNRs acquired from (a) GNRs without centrifugation and (b) the purified GNRs for different reacting time with $Na_2S_2O_3$.

with increasing the mixing time of the GNRs and $Na_2S_2O_3$, as shown in Figure 3(a). As expected, the GNRs possess two principal plasmon absorption bands, a weak transverse plasmon resonance band at 520 nm, and a strong longitudinal plasmon resonance (LPR) band at 765 nm. After adding the excessive $Na_2S_2O_3$ to the GNRs solution, the LPR band red-shifts immediately from 765 nm to 792 nm within 5 minutes due to the fact that the chalcogenide layer was coated on surface of GNRs, while transverse plasmon resonance band red-shifts only several nanometers, as shown in the curves A–C of Figure 3(a). Furthermore, the curves (D–F) in Figure 3(a) also clearly show that the LPR bands have a bit of blue shifts with increasing the reaction time of the original GNRs. This is because there is a slight change of the aspect ratio of the core-shell nanorods during the first 13 minutes. Additionally, the more vigorous reaction of the GNRs and $Na_2S_2O_3$ may occur in the mixture solution when the reaction temperature reached 50°C after heating

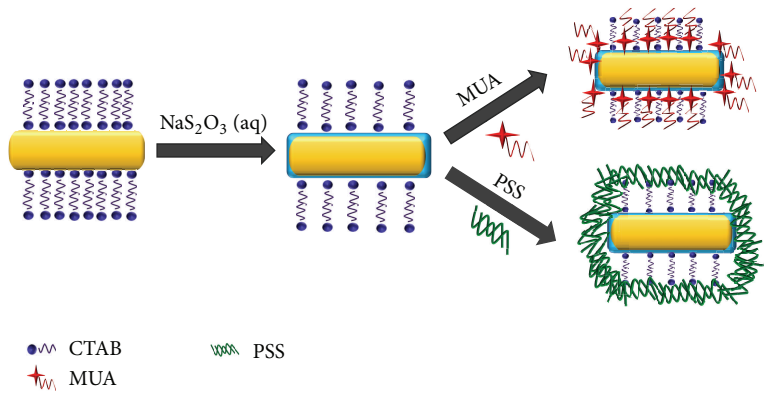

Figure 4: Schematic illustration of functionalization of Au_2S/AuAgS/GNRs.

for 13 minutes, which results in the blue shifts of the LPR bands, which was shown in the curves G–J of Figure 3(a). In particular, for the case of curves K in Figure 3(a), the LPR band suffered a significant blue shift as well as a dramatically decline of the spectrum intensity. The distinct change of LPR bands is ascribed to the continuous corrosion of $Na_2S_2O_3$ which makes the average length and diameter of the GNRs naturally decreased, further resulting in the decrease of the aspect ratio of the GNRs. Therefore, the above shift of LPR bands is different from the consecutive red shifts of the LPR bands with increasing the reaction time which was described in [27].

It is well known that the as-synthesized GNRs are encapsulated with CTAB which shapes and stabilizes the nanorods [29]. In fact, the excess CTAB in the GNRs solution is detrimental to the synthesis of core-shell nanorods such as the Au/Ag and Au/SiO_2 nanorods [20, 30]. However, as shown in Figure 3(b), when the purified GNRs reacted with the $Na_2S_2O_3$, the LPR band of Au_2S/AuAgS/GNRs had only blue shifts no matter for how long was the reaction carried out. Compared with the case of GNRs without centrifugation, the LPR bands in Figure 3(b) have no red shift during the process of mixing the GNRs and $Na_2S_2O_3$. It is indicated that the CTAB plays an important role in tuning the LPR band to near-infrared and slowing down the dramatic blue shifts because the CTAB as a blocking agent stopped the $Na_2S_2O_3$ molecular directly contacting with the surface of GNRs.

3.2. Functionalization of Au_2S/AuAgS/GNRs with PSS and MUA. In general, during the preparation of GNRs and Au_2S/AuAgS/GNRs, the CTAB as a surfactant is coated on the surface of the nanorods. However, the CTAB has significant cytotoxicity to the biological tissue and blocks the nanorods to bind biological molecules. So the functionalized modification of the nanorods is important for their applications. In our research, MUA and PSS molecules are chosen as the modifier to functionalize the Au_2S/AuAgS/GNRs. The scheme of MUA and PSS functionalized with Au_2S/AuAgS/GNRs is illustrated in Figure 4. As described in Section 2.4, the MUA-capped and PSS-capped Au_2S/AuAgS/GNRs are, respectively, centrifuged and redispersed in water to remove free CTAB and the excessive MUA/PSS. Then, for the functionalized

Table 1: ξ-potential of Au_2S/AuAgS/GNRs solution.

	ξ-potential (mV)
GNRs	51
Au_2S/AuAgS/GNRs	30.6
MUA/Au_2S/AuAgS/GNRs	37.2
PSS/Au_2S/AuAgS/GNRs	−44.3

Au_2S/AuAgS/GNRs, the displacement of CTAB to MUA/PSS was monitored by ξ-potential measurement. As shown in Table 1, the GNRs and Au_2S/AuAgS/GNRs coated with CTAB are positively charged during the preparation of GNRs. However, after coating MUA layer on the surface of Au_2S/AuAgS/GNRs, the zeta-potential increases 6.6 mV more than that of Au_2S/AuAgS/GNRs due to the thiol group attached to the nanorods and the formation of layers of alkanethiol molecules [31, 32]. Meanwhile, the zeta-potential of PSS suffers an extreme change from +30.6 mV to −44.3 mV, which was from the interaction between the positive charge of CTAB and the negative charge of PSS [33, 34]. It is because the electrostatic interaction between the anionic SO_3 groups of PSS and the trimethylammonium headgroup of CTAB results in the extreme change in the ξ-potential which switched from positive to negative [35].

The optical properties of the functionalized layers coated on the surface of Au_2S/AuAgS/GNRs were also characterized by UV-vis-NIR absorption spectroscopy. As shown in Figure 5, the LSP bands of Au_2S/AuAgS/GNRs and the functionalized Au_2S/AuAgS/GNRs are located in 802, 807, and 798 nm, respectively. Comparing with Au_2S/AuAgS/GNRs, the LSP band of MUA-capped Au_2S/AuAgS/GNRs has 5 nm red shift but the one of PSS-capped Au_2S/AuAgS/GNRs has 4 nm blue shift. The above shifts can be attributed to the changes of refractive index caused by replacing CTAB with MUA/PSS molecules in the vicinity of the Au_2S/AuAgS/GNRs [31, 32], as shown in the variations of ξ-potentials of the functionalized Au_2S/AuAgS/GNRs in Table 1. It further confirms that the functionalization of Au_2S/AuAgS/GNRs with PSS and MUA has been achieved, which not only diminishes the cytotoxicity of CTAB but also makes Au_2S/AuAgS/GNRs easy to attach with biomarker

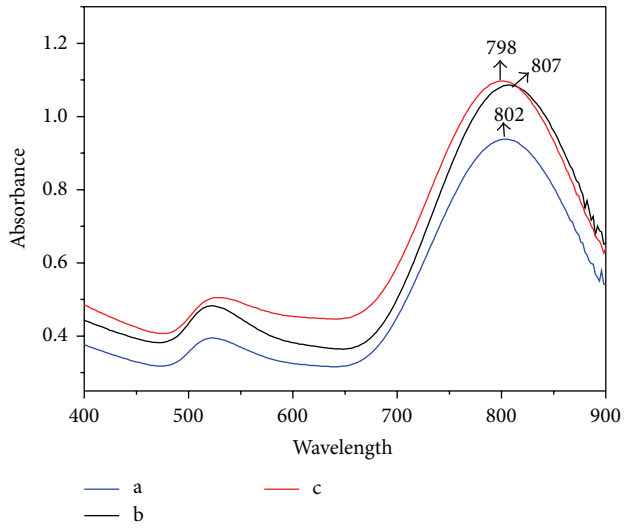

Figure 5: UV-vis-NIR spectra of Au_2S/AuAgS/GNRs (curve a), PSS-capped Au_2S/AuAgS/GNRs (curve b), and MUA-capped Au_2S/AuAgS/GNRs (curve c).

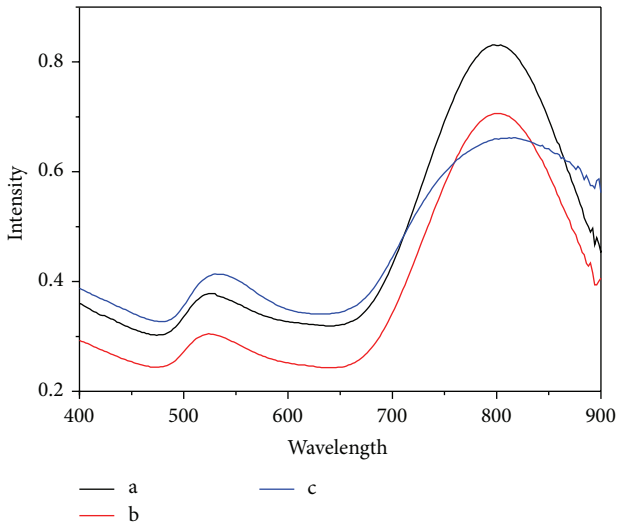

Figure 6: UV-vis-NIR spectra of MUA-capped Au_2S/AuAgS/GNRs (curve a), MUA-capped Au_2S/AuAgS/GNRs conjugated with anti-PSA antibody (curve b), and MUA-capped Au_2S/AuAgS/GNRs conjugated with anti-PSA antibody and PSA (curve c).

molecules as biosensing probes for the biological detection later.

3.3. Application of Au_2S/AuAgS/GNRs Immune Probes. As an immunoassay application, the prepared MUA-capped Au_2S/AuAgS/GNRs were conjugated with the anti-PSA antibody to form the immune probe for specific binding with PSA to monitor early prostate cancer [36]. Before attaching anti-PSA antibody, the EDC and NHS biomolecules as the coupling agents were added to the MUA-capped Au_2S/AuAgS/GNRs solution so that the EDC/NHS-terminated nanorods are easy to covalently attach with the anti-PSA antibody. As shown in Figure 6, the absorption spectrum of MUA-capped Au_2S/AuAgS/GNRs conjugated with anti-PSA antibody showed an obvious decrease of intensity and a slight red shift of the LSP band. After adding 10 μL of 0.04 mg/mL PSA to 5 mL of the immune probe solution, the LSP band of the immune probe incubated with PSA was further declined and broadened to a longer wavelength. It is believed that the above results come from the specific binding of PSA with the anti-PSA antibody of the immune probes.

In addition, the PSS-capped Au_2S/AuAgS/GNRs were also employed to perform the immunoassay with the above protocol. However, after adding the anti-PSA antibody into the PSS-capped Au_2S/AuAgS/GNRs solution, there was no shift of the LSP band of the nanorods solution. It indicated that the anti-PSA antibody might not be attached on the PSS-capped nanorods. In other words, the PSS-capped Au_2S/AuAgS/GNRs do not act as the immune probes to detect PSA. But the PSS-coated Au_2S/AuAgS/GNRs may be useful to detect other biomolecules by binding with the corresponding target analytes. Therefore, the different biorecognition driven by the MUA-capped and PSS-capped Au_2S/AuAgS/GNRs immune probes reveals a good selectivity of biomolecules by functional Au_2S/AuAgS/GNRs, which may be an important capability for multiplex biosensor.

4. Conclusion

In summary, we have successfully synthesized Au_2S/AuAgS-coated gold nanorods in a simple and efficient way. And CTAB plays an important role in controlling the corrosion rate of GNRs, leading to different changes of LSP band of the nanocomposites. With excessive CTAB molecular in GNRs solution, the LSP peak of the as-prepared Au_2S/AuAgS GNRs firstly red-shifts and then blue-shifts as the reaction time between $Na_2S_2O_3$ and GNRs increases. After removig the excessive CTAB by centrifugation, the purified GNRs were mixed with the $Na_2S_2O_3$ solution; the LSP peak only tends to blue-shift. Moreover, the MUA- and PSS-coated Au_2S/AuAgS GNRs exhibit different chemical reaction mechanisms, which are achieved by thiol group bonding and electrostatic interaction, respectively. Experimentally, it demonstrated that the MUA-coated Au_2S/AuAgS GNRs can be prepared as immune nanoprobes conjugated with anti-PSA antibody to detect PSA because its LSP band has red shift and broadening accompanied with an intensity decrease. In principle, the Au_2S/AuAgS GNRs as an effective nanoprobe may be extended to assay other biomarkers based on their LSPR properties in NIR region.

Conflict of Interests

The authors declare that there is no conflict of interests regarding the publication of this paper.

Acknowledgments

This work was supported by the National Natural Science Foundation of China (Grant nos. 61275153, 21377063, 61335011, and 61320106014), the Natural Science Foundation of Zhejiang (Grant no. LY12A04002), the Natural Science Foundation of Ningbo (Grant nos. 2012A610107 and 2014A610106), and K. C. Wong Magna Foundation of Ningbo University, China.

References

[1] P. V. Kamat, "Photophysical, photochemical and photocatalytic aspects of metal nanoparticles," *The Journal of Physical Chemistry B*, vol. 106, no. 32, pp. 7729–7744, 2002.

[2] K. L. Kelly, E. Coronado, L. L. Zhao, and G. C. Schatz, "The optical properties of metal nanoparticles: the influence of size, shape, and dielectric environment," *Journal of Physical Chemistry B*, vol. 107, no. 3, pp. 668–677, 2003.

[3] S. M. Marinakos, S. Chen, and A. Chilkoti, "Plasmonic detection of a model analyte in serum by a gold nanorod sensor," *Analytical Chemistry*, vol. 79, no. 14, pp. 5278–5283, 2007.

[4] J. V. Jokerst, A. J. Cole, D. van de Sompel, and S. S. Gambhir, "Gold nanorods for ovarian cancer detection with photoacoustic imaging and resection guidance via raman imaging in living mice," *ACS Nano*, vol. 6, no. 11, pp. 10366–10377, 2012.

[5] S. J. Guo, L. Wang, Y. Y. Wang, Y. X. Fang, and E. K. Wang, "Bifunctional Au@Pt hybrid nanorods," *Journal of Colloid and Interface Science*, vol. 315, no. 1, pp. 363–368, 2007.

[6] P. Zijlstra, J. W. M. Chon, and M. Gu, "Five-dimensional optical recording mediated by surface plasmons in gold nanorods," *Nature*, vol. 459, no. 7245, pp. 410–413, 2009.

[7] J. W. M. Chon, C. Bullen, P. Zijlstra, and M. Gu, "Spectral encoding on gold nanorods doped in a silica sol-gel matrix and its application to high-density optical data storage," *Advanced Functional Materials*, vol. 17, no. 6, pp. 875–880, 2007.

[8] N. R. Jana, L. Gearheart, and C. J. Murphy, "Wet chemical synthesis of high aspect ratio cylindrical gold nanorods," *The Journal of Physical Chemistry B*, vol. 105, no. 19, pp. 4065–4067, 2001.

[9] A. Gole and C. J. Murphy, "Seed-mediated synthesis of gold nanorods: role of the size and nature of the seed," *Chemistry of Materials*, vol. 16, no. 19, pp. 3633–3640, 2004.

[10] R.-D. Jean, W.-D. Cheng, M.-H. Hsiao, F.-H. Chou, J.-S. Bow, and D.-M. Liu, "Highly electrostatically-induced detection selectivity and sensitivity for a colloidal biosensor made of chitosan nanoparticle decorated with a few bare-surfaced gold nanorods," *Biosensors and Bioelectronics*, vol. 52, pp. 111–117, 2014.

[11] S. Yao, H.-H. Cai, M. Liu, and P.-H. Yang, "Fluorescent labeling of cellular targets and multicolor imaging with gold nanorods," *Dyes and Pigments*, vol. 101, pp. 286–294, 2014.

[12] A. M. Alkilany, L. B. Thompson, S. P. Boulos, P. N. Sisco, and C. J. Murphy, "Gold nanorods: their potential for photothermal therapeutics and drug delivery, tempered by the complexity of their biological interactions," *Advanced Drug Delivery Reviews*, vol. 64, no. 2, pp. 190–199, 2012.

[13] J.-M. Liu, X.-X. Wang, F.-M. Li et al., "A colorimetric probe for online analysis of sulfide based on the red shifts of longitudinal surface plasmon resonance absorption resulting from the stripping of gold nanorods," *Analytica Chimica Acta*, vol. 708, no. 1-2, pp. 130–133, 2011.

[14] V. Canpean, A. M. Gabudean, and S. Astilean, "Enhanced thermal stability of gelatin coated gold nanorods in water solution," *Colloids and Surfaces A: Physicochemical and Engineering Aspects*, vol. 433, pp. 9–13, 2013.

[15] C. J. Murphy, T. K. Sau, A. M. Gole et al., "Anisotropic metal nanoparticles: synthesis, assembly, and optical applications," *Journal of Physical Chemistry B*, vol. 109, no. 29, pp. 13857–13870, 2005.

[16] X. Huang, S. Neretina, and M. A. El-Sayed, "Gold nanorods: from synthesis and properties to biological and biomedical applications," *Advanced Materials*, vol. 21, no. 48, pp. 4880–4910, 2009.

[17] J. Pérez-Juste, I. Pastoriza-Santos, L. M. Liz-Marzán, and P. Mulvaney, "Gold nanorods: synthesis, characterization and applications," *Coordination Chemistry Reviews*, vol. 249, no. 17-18, pp. 1870–1901, 2005.

[18] C. J. Murphy, T. K. Sau, A. Gole, and C. J. Orendorff, "Surfactant-directed synthesis and optical properties of one-dimensional plasmonic metallic nanostructures," *MRS Bulletin*, vol. 30, no. 5, pp. 349–355, 2005.

[19] T. K. Sau and C. J. Murphy, "Seeded high yield synthesis of short Au nanorods in aqueous solution," *Langmuir*, vol. 20, no. 15, pp. 6414–6420, 2004.

[20] Y. Xiang, X. Wu, D. Liu et al., "Gold nanorod-seeded growth of silver nanostructures: from homogeneous coating to anisotropic coating," *Langmuir*, vol. 24, no. 7, pp. 3465–3470, 2008.

[21] R. Yasukuni, K. Ouhenia-Ouadahi, L. Boubekeur-Lecaque et al., "Silica-coated gold nanorod arrays for nanoplasmonics devices," *Langmuir*, vol. 29, no. 41, pp. 12633–12637, 2013.

[22] J. N. Anker, W. P. Hall, O. Lyandres, N. C. Shah, J. Zhao, and R. P. Van Duyne, "Biosensing with plasmonic nanosensors," *Nature Materials*, vol. 7, no. 6, pp. 442–453, 2008.

[23] X. Huang, I. H. El-Sayed, W. Qian, and M. A. El-Sayed, "Cancer cell imaging and photothermal therapy in the near-infrared region by using gold nanorods," *Journal of the American Chemical Society*, vol. 128, no. 6, pp. 2115–2120, 2006.

[24] H. Kang, S. Jeong, Y. Park et al., "Near-infrared SERS nanoprobes with plasmonic Au/Ag hollow-shell assemblies for in vivo multiplex detection," *Advanced Functional Materials*, vol. 23, no. 30, pp. 3719–3727, 2013.

[25] B. D. Busbee, S. O. Obare, and C. J. Murphy, "An improved synthesis of high-aspect-ratio gold nanorods," *Advanced Materials*, vol. 15, no. 5, pp. 414–416, 2003.

[26] R. C. Wadams, L. Fabris, R. A. Vaia, and K. Park, "Time-dependent susceptibility of the growth of gold nanorods to the addition of a cosurfactant," *Chemistry of Materials*, vol. 25, no. 23, pp. 4772–4780, 2013.

[27] H. Huang, X. Liu, Y. Zeng et al., "Optical and biological sensing capabilities of Au_2S/AuAgS coated gold nanorods," *Biomaterials*, vol. 30, no. 29, pp. 5622–5630, 2009.

[28] H. Huang, X. Liu, B. Liao, and P. K. Chu, "A localized surface plasmon resonance biosensor based on integrated controllable Au_2S/AuAgS-coated gold nanorods composite," *Plasmonics*, vol. 6, no. 1, pp. 1–9, 2011.

[29] S. Lee, L. J. E. Anderson, C. M. Payne, and J. H. Hafner, "Structural transition in the surfactant layer that surrounds gold nanorods as observed by analytical surface-enhanced raman spectroscopy," *Langmuir*, vol. 27, no. 24, pp. 14748–14756, 2011.

[30] C. C. Huang, C. H. Huang, I. T. Kuo, L. K. Chau, and T. S. Yang, "Synthesis of silica-coated gold nanorod as Raman tags

by modulating cetyltrimethylammonium bromide concentration," *Colloids and Surfaces A: Physicochemical and Engineering Aspects*, vol. 409, pp. 61–68, 2012.

[31] Q. Huo, J. Colon, A. Cordero et al., "A facile nanoparticle immunoassay for cancer biomarker discovery," *Journal of Nanobiotechnology*, vol. 9, article 20, 2011.

[32] Y. Ma, J. Zhou, W. Zou, Z. Jia, L. Petti, and P. Mormile, "Localized surface plasmon resonance and surface enhanced raman scattering responses of Au@Ag core-shell nanorods with different thickness of Ag shell," *Journal of Nanoscience and Nanotechnology*, vol. 14, no. 6, pp. 4245–4250, 2014.

[33] C. X. Yu and J. Irudayaraj, "Multiplex biosensor using gold nanorods," *Analytical Chemistry*, vol. 79, no. 2, pp. 572–579, 2007.

[34] C. G. Wang, Y. Chen, T. T. Wang, Z. F. Ma, and Z. M. Su, "Biorecognition-driven self-assembly of gold nanorods: a rapid and sensitive approach toward antibody sensing," *Chemistry of Materials*, vol. 19, no. 24, pp. 5809–5811, 2007.

[35] Y. N. Ma, J. Zhou, L. Shu, T. H. Li, L. Petti, and P. Mormile, "Optimizing Au/Ag core-shell nanorods: purification, stability, and surface modification," *Journal of Nanoparticle Research*, vol. 16, no. 6, article 2439, 10 pages, 2014.

[36] X. Liu, Q. Dai, L. Austin et al., "A one-step homogeneous immunoassay for cancer biomarker detection using gold nanoparticle probes coupled with dynamic light scattering," *Journal of the American Chemical Society*, vol. 130, no. 9, pp. 2780–2782, 2008.